Gisborne District Council
Tsunami Inundation Study

Xiaoming Wang
William Power
Hannah Brackley
Gegar Prasetya
Biljana Lukovic
Kelvin Berryman

GNS Science Consultancy Report 2009/233
September 2009

GNS SCIENCE
TE PŪ AO

CONFIDENTIAL

BIBLIOGRAPHIC REFERENCE

Wang, X.; Prasetya, G.; Power, W.; Lukovic, B.; Brackley, H.; Berryman, K. 2009. Gisborne District Council Tsunami Inundation Study, *GNS Science Consultancy Report* 2009/233 130 p.

CONTENTS

FIGURES

TABLES

EXECUTIVE SUMMARY

Gisborne District Council contracted GNS Science to conduct inundation modelling of Poverty Bay and Wainui Beach under a set of tsunami scenarios. The scenarios include tsunami caused by both local and distant earthquake sources. The likelihood of these scenarios was to be assessed, so that they could be used to inform evacuation planning.

The distant source scenarios were chosen to represent, as closely as possible, the extent of the 100 year and 500 year inundations caused by distant source tsunami. Using the methodology of Berryman (2005) appropriate sources were chosen to be earthquakes on the Peru coast of magnitude M_W 9.1 and M_W 9.4.

The local source scenarios were selected from the Hikurangi margin earthquake scenarios studied by Power et al (2008), and from the fault sources offshore of Poverty Bay identified in the New Zealand seismic hazard model.

The study region for the inundation modelling consists of the interior of Poverty Bay plus the Wainui Beach coast. Within Poverty Bay a greater focus has been placed on the developed areas of Gisborne city, and on the Muriwai area where inundation was found under many scenarios.

The impact on Poverty Bay of the estimated 100 year distant-source inundation is quite similar to that of the 1960 Chile tsunami (the worst distant source event of the past century), which provides an approximate validation of our methods.

In Gisborne the 100 year inundation from distant sources is confined mostly to the fringes of the port area and the Turanganui river mouth, while the 500 year inundation is estimated to have a wider impact on the coastal suburbs, the port areas, and on low-lying areas close to rivers. Muriwai, on the southwest of Poverty Bay, is estimated to be particularly badly hit in such an event.

There are many possible local sources of tsunami that could affect the Poverty Bay region. Some of these sources are earthquakes that rupture the interface between the Australian and Pacific continental plates, others are earthquakes that rupture faults that lie within the overlying Australian plate or the subducting Pacific plate. Earthquakes that rupture on both the plate interface and simultaneously on faults within the crust of the Australian plate are also a possibility. Tsunami may also be caused by submarine landslides that occur near the edge of the continental shelf, but these are not studied in this report.

We have modelled a selection of these earthquake scenarios which provides a representative sample of the different types of events that could take place. For each local source scenario we estimated the vertical seabed deformation, which is the primary source of the tsunami waves. Using the COMCOT program, we have modelled the propagation of these waves to the coast and the subsequent inundation of the land in Poverty Bay and Wainui. For the distant sources, a combination of the MOST and COMCOT programs were used.

Mean tide level has been used unless otherwise stated; higher water levels will occur at high tide, and additional modelling at high tide was conducted for some scenarios.

Estimating the return time for tsunami inundation is a very difficult process requiring a comprehensive set of models for all the scenarios which contribute to the tsunami hazard on the time scales of interest, and a model for the probabilities of each scenario. The set of local source scenarios modelled for this study, and their recurrence interval estimates, are not sufficient to perform such an analysis in a systematic way.

The inundation caused by local sources can be very specific to the details of the source, and these details are usually not known with confidence. Most of the scenarios used in this report assume earthquake ruptures with uniform slip (i.e. uniform amount of dislocation on the fault plane segments). Some are based on GPS coupling models which allow for smooth variations in slip. In actual ruptures, the slip on the fault plane varies in dislocation in complicated ways on a variety of spatial scales. The pattern of slip distribution cannot currently be predicted with any confidence. The pattern of slip distribution can affect the resulting tsunami. Our assumed uniform slip distribution may represent an approximate 'average' event compared to real earthquakes of the same magnitude which may have larger slip in some areas and lesser slip in others.

The Muriwai area was inundated in several of the scenarios. The low, flat landscape and the low height of the dunes at the coast provide little resistance to approaching tsunami. Near Gisborne city the coastal dune is higher, and this provides a substantial degree of protection. Inundation is most likely to occur around the Turanganui river mouth, the port area, and near gaps in the sand dune. Only in the most severe scenario is the coastal sand dune widely overtopped. In Wainui the height of the steep beach face appears to provide protection in many of the scenarios, although the lower-lying areas surrounding the creeks were often inundated. The worst scenario for Wainui was an earthquake in the outer rise of the Pacific plate, whereas within Poverty Bay the most severe scenario was one of a large earthquake on the plate interface.

The LIDAR data used to define the topographic modelling grids may possibly include the elevation of bridge decks in some instances. Since tsunami waves may in practise flow under the bridge, our model may under-represent the true extent of up-river flooding in these cases.

1.0 INTRODUCTION

Gisborne District Council contracted GNS Science to conduct inundation modelling of Poverty Bay and Wainui Beach under a set of tsunami scenarios. The scenarios include tsunami caused by both local and distant earthquake sources. The likelihood of these scenarios was to be assessed, so that they could be used to inform evacuation planning.

The distant source scenarios were chosen to represent, as closely as possible, the 100 year and 500 year inundations caused by distant source tsunami. Using the methodology of Berryman (2005) appropriate sources were chosen to be earthquakes on the Peru coast of magnitude M_W 9.1 and M_W 9.4.

The local source scenarios were selected from the Hikurangi margin earthquake scenarios studied by Power et al (2008), and from the fault sources offshore of Poverty Bay identified in the New Zealand seismic hazard model.

The study region for the inundation modelling consists of the interior of Poverty Bay plus the Wainui Beach coast. Within Poverty Bay a greater focus has been placed on the developed areas of Gisborne city, and on the Muriwai area where inundation was found under many scenarios.

Inundation models were conducted assuming a mean sea level. In addition, selected sources of particular interest were modelled under the assumption of a high tide. This was approximated by adding a fixed increment to the mean sea level and allowing tsunami to propagate and interact with the coastal region at this increased water level over the entire duration of a simulation. In addition, the uplift or subsidence of land and seabed caused by earthquakes was also taken into account in the numerical study of inundation.

2.0 BACKGROUND

In recorded history Gisborne has been affected by distant source tsunami on at least three occasions: in 1868 (M_W 9.1 earthquake in Peru), 1877 (M_W 9.0 earthquake in northern Chile), and 1960 (M_W 9.5 earthquake in southern Chile). Gisborne was also hit by two local source tsunami which both occurred in 1947 (M_W 7.1 and M_W 6.9 earthquakes offshore of the Raukumara peninsula).

Public awareness of tsunami has been high since the 2004 Indian Ocean Tsunami. This awareness is particularly high in Gisborne because of the three tsunami that occurred within living memory (two in 1947, and one in 1960). The self-evacuation of local residents in response to the earthquakes of 4 May 2006 and 20 December 2007 is evidence of this.

3.0 OBJECTIVE

The primary objective of this project is to produce plots of the inundation extent and flow-depths in Poverty Bay and Wainui for a variety of scenario tsunami events. These scenarios

include approximations to the 100 year and 500 year distant-source tsunami, as well as selected local-source scenarios.

4.0 METHOD

4.1 Numerical Model

Numerical modelling is a very effective approach to studying the hazards of tsunami, especially for potential events in the future. Since the devastating 2004 Indian Ocean Tsunami, many numerical models have been improved or newly developed to efficiently and accurately study the generation, propagation, runup and inundation of tsunami. In this study, one of the most widely used tsunami models in the world, COMCOT (COrnell Multi-grid COupled Tsunami model) is adopted to investigate the runup and inundation of potential tsunami generated from local and distant sources.

COMCOT was developed for modelling long waves in the ocean, particularly tsunami, by the wave research group in the Department of Civil & Environmental Engineering of Cornell University, USA in the early 1990's. This model is capable of studying the entire life span of tsunami including its generation, propagation, runup and inundation. With the implementation of nested grids, the model can use a relatively larger grid resolution to efficiently simulate the propagation of tsunamis in the deep ocean and then switch to apply finer grid resolutions in coastal regions to account for the shortening of tsunami waves due to the shallowness of water. In this approach, the computational efficiency and the numerical accuracy can be well balanced.

This model has been systematically validated and has consistently shown its satisfactory accuracy when running against analytical solutions (Liu, Cho and Fujima, 1994; Cho, 1995), experimental studies (Liu, Cho and Fujima, 1994; Liu, et al., 1995; Cho, 1995) and benchmark problems in the 3rd International Long Wave Workshop in 2003 (Wang, Orfila and Liu, 2008). And it has been successfully applied to study the propagation, runup and inundation of several historical events including the 1960 Chilean Tsunami (Liu, et al., 1994), the 1986 Taiwan Hualien Tsunami (Liu, et al., 1998), the 2005 Algerian Tsunami (Wang and Liu, 2005) and the 2004 Indian Ocean Tsunami (Wang and Liu, 2006, 2007, 2008), and demonstrated satisfactory achievements in comparison with either field or satellite observations and tidal gauge measurements. It has also been applied to study the flooding and tsunami forces on structures in the cities of Galle, Matara and Hambantota in Sri Lanka for building code suggestions (Wijetunge, Wang and Liu, 2008) and the tsunami hazards and early warning system in South China Sea (Liu, Wang and Salisbury, 2009).

In some of the scenarios for this study the effect of tsunami occurring at high-tide was modelled. This was approximated by adding a fixed increment (i.e. half the tidal range of 1.5m for Poverty Bay) to the baseline water-level. In these scenarios, the generated tsunami propagates and interacts with coastal areas at this increased water level.

4.2 Model Grids

It is well known that as tsunami approaches coastal regions from the deep ocean, its wave length becomes shorter and the amplitude becomes larger due to the shallowness of water in

comparison with those in the deep ocean. To account for this effect, three levels of bathymetric/topographic data resolution were implemented for the numerical simulations 250 metres, 50 metres and 10 metres, derived from the raw data set described in Section 5.0.

The first-level grids cover the entire region of Hawke Bay, Poverty Bay and local fault zones where future earthquakes could generate tsunami potentially threatening the Gisborne area, including the Hikurangi Trough where the Pacific Plate is subducting beneath the Australian Plate (Figure 4.2-1).

The second-level grid covers the entire Poverty Bay and a significant portion of continental shelf southwest of Poverty Bay with 50-meter grid resolution. The water depth in most areas of this grid region is usually shallower than 100 meters (Figure 4.2-2).

The third-level grid covers the entire Poverty Bay and Gisborne City area with 10 meter grid resolution (Figure 4.2-3). This high resolution bathymetric and topographical data was derived from LINZ nautical charts and LIDAR data, and is used to catch the fine details of runup and inundation in the Gisborne area for potential tsunami events.

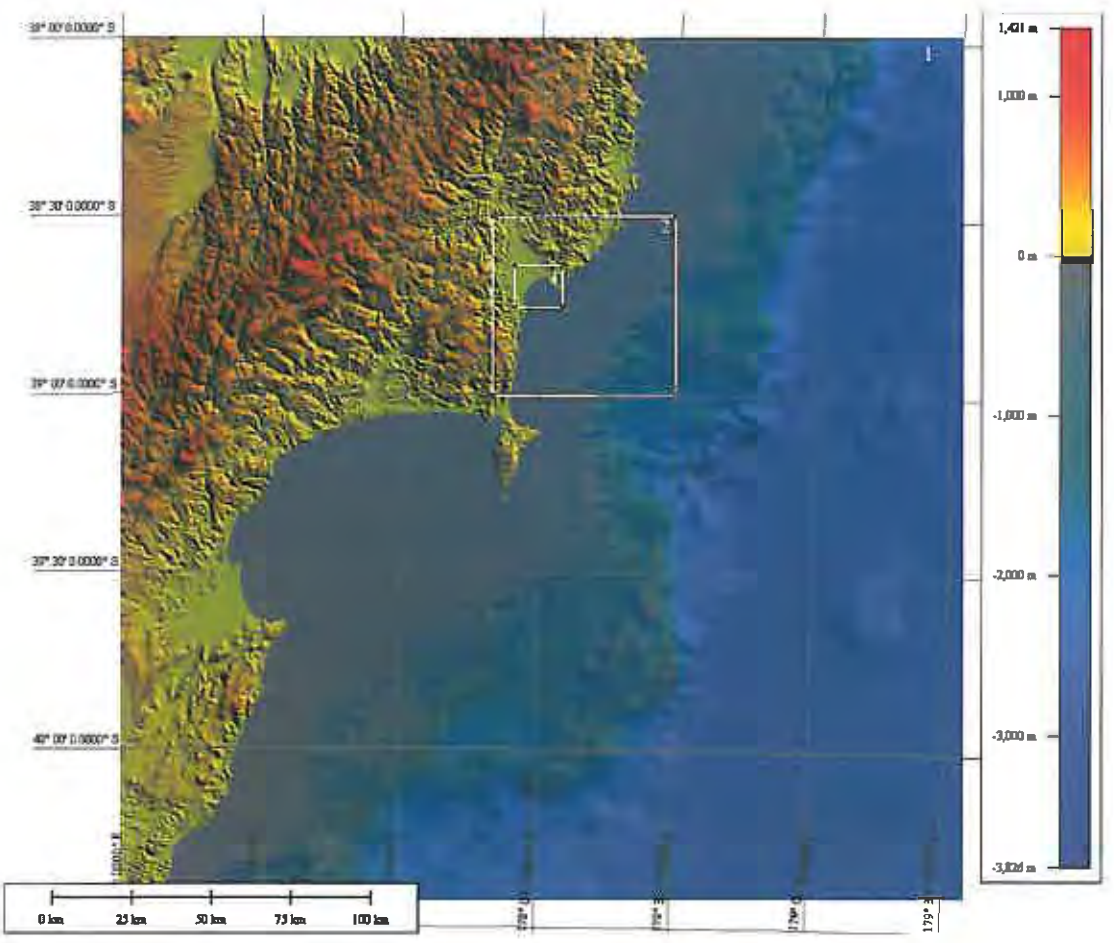

Figure 4.2-1 The first-level grid covers the entire Hawke Bay, Poverty Bay and local faults which may trigger tsunami threats to Gisborne area. The grid resolution is 250 meters.

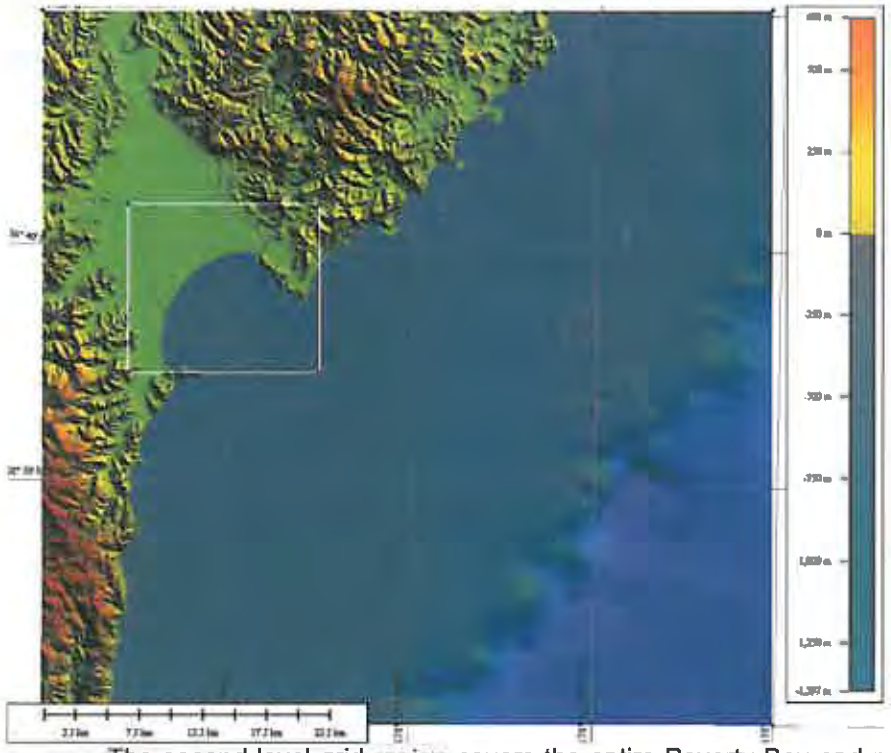

Figure 4.2-2 The second-level grid region covers the entire Poverty Bay and nearby coastal area with a grid resolution of 50 meters.

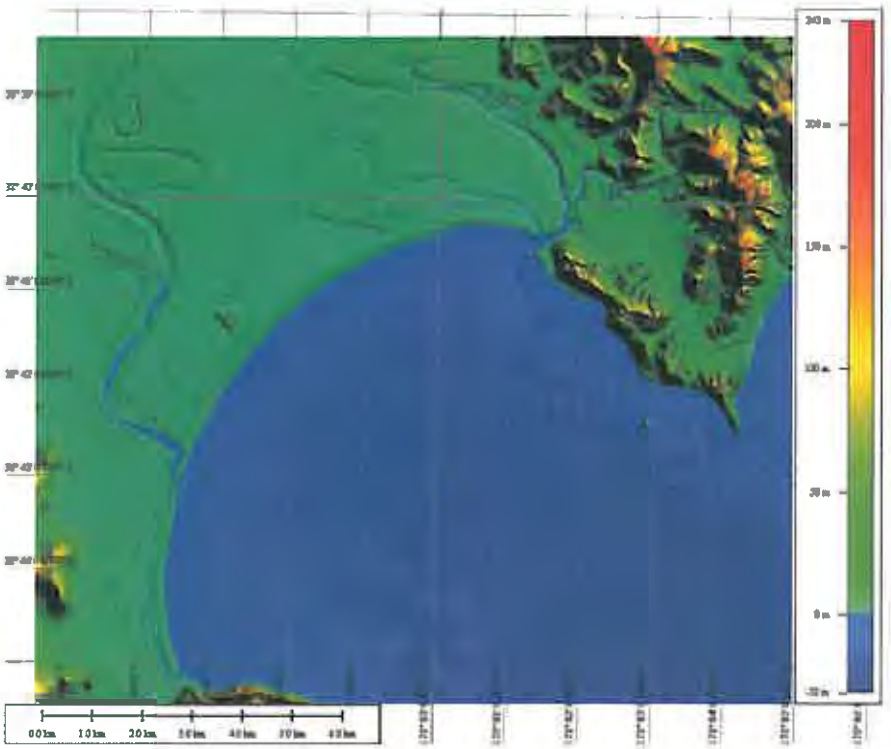

Figure 4.2-3 The third-level grid region covers the interior of Poverty Bay plus Wainui Beach with a grid resolution of 10 meters.

4.3 Roughness Coefficient

The characteristics of bathymetric and topographic features along with the friction of the land surface control the extent of inundation further inland. The numerical model COMCOT uses the Manning roughness coefficient *n* as a friction coefficient to represent these features. This coefficient can be used as a single value for the entire region or vary according to the bathymetric and topographic (land cover) characteristics. Coastal features such as sand dunes, cliffs, river mouths and channels or inlets, and vegetation cover as well as residential and industrial areas notably affect the extent of inundation further inland. In this project, variable Manning roughness coefficients are used based on the land use classes, LIDAR ground striking data, and aerial photographs. The friction coefficient value for each land use class is derived from published literature on inundation modelling and flood risk and damage assessment studies (van der Sande et al., 2003; Imamura et al, 2006; Murashima et al., 2008), and normalised to the COMCOT Manning roughness coefficient used for the ocean part as listed in Table 1. Applications of this coefficient to the most important part of Gisborne including the Wainui region are illustrated in Figure 4.3-1.

Table 4.3-1 Manning roughness coefficient

Land Use Conditions	Manning roughness coefficient n (sec/m$^{1/3}$)
Oceans, Rivers	0.013
Pavement ground (industrial area, township/city, road)	0.015
Arable land (including waste land, open field)	0.016 - 0.022
Woodland (including orchard, grass, bushes, low density forest areas, farm)	0.025 – 0.027
Low density residential areas (building density < 30%)	0.028
Mid density residential areas (building density 30 - 50%)	0.03
High density residential areas (building density > 50%)	0.032
Buildings (residential/industrials)	0.2

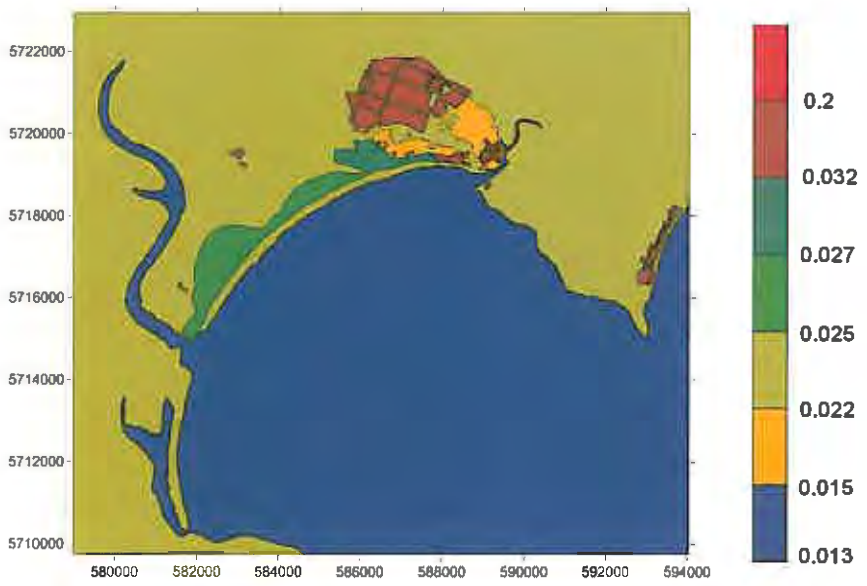

Figure 4.3-1 The Manning roughness coefficient distribution based on land cover (land use classes). Scale bar unit is in sec/m $^{1/3}$

5.0 DATA

One of the basic inputs into the tsunami modelling is the combined elevation and bathymetry model. The model was generated in ARCINFO using the TOPOGRID function from the following data sets:

- LiDAR data supplied by Gisborne District EMO;
- Contours and spot heights from LINZ 1:50,000 Topographic database in the areas not covered by LiDAR;
- Bathymetry contours and soundings digitised from LINZ Nautical Charts, including the C-Map dataset supplied by Seabed Mapping of Nelson.

All elevation and bathymetry data was projected to UTM Zone 60S projection and all heights and depths were measured in terms of Mean Sea Level. A nest of three grids with different resolution was produced:

- 5 m grid covering the Poverty Bay area (approximately 157 km^2);
- 25 m grid covering surrounding area of approximately 4,000 km^2;
- 125 m grid covering an area of over 74,000 km^2) and including the location of tsunami sources.

The grids were converted to gridded points and exported into ASCII format to be used in the COMCOT Tsunami Model. COMCOT processed this input data to produce the model grids described in Section 4.2 (note the change in resolution).

6.0 SOURCES

The Gisborne region faces a range of distant and local tsunami sources. The historic record of distant-source tsunami in this region is dominated by events originating in South America (in 1868, 1877, 1960). Several other large earthquakes occurred on the South American coast in the period before European colonisation of New Zealand, and some of these are likely to have affected the Poverty Bay area too.

Other distant source regions that might have an impact on the Gisborne region include Central America, Cascadia (NW United States), Alaska and the Aleutian arc.

Within the southwest-Pacific region, excluding New Zealand, there are potential tsunami sources on the Kermadec arc[1], the Vanuatu – Fiji arc, and near the Solomon Islands. None of these is well orientated to direct tsunami energy towards the Poverty Bay region, and in most cases large earthquakes on these sources will pose a risk only to beach users and small boat users due to strong surges of water - they are unlikely to be big enough to cause notable inundation in the Gisborne region.

Local tsunami sources are largely those associated with the Hikurangi subduction zone. This includes the interface between the Australian and Pacific plates, as well as associated splay faults such as the Lachlan fault, and outer-rise earthquakes caused by buckling of the subducting plate.

[1] The southern end of the Kermadec arc, from about 36°S southwards, is a local tsunami source for the Gisborne region and might pose an inundation threat.

The two 1947 tsunami appear to have been caused by a special category of 'tsunami-earthquakes' that have weak shaking, and are associated with seamounts that are being subducted below the Australian plate (Bell et al., 2008). Such events may be relatively common around the Raukumara peninsular, and perhaps elsewhere in the Hikurangi margin. These events may relieve stress on the plate interface in such a way that the frequency of conventional plate-interface earthquakes is reduced.

Bathymetry of the offshore Poverty Bay area shows evidence of many past submarine landslides. In most cases it is not possible to date these events, which makes it difficult to estimate the frequency with which such events occur. The 20 December 2007 Gisborne earthquake produced strong ground shaking in this area, but caused no tsunamigenic landslides. Further north, offshore of the Raukumara Peninsula there is evidence of a very large submarine landslide (Collot et al., 2001) which may have been triggered by a subducting seamount, fortunately such events appear to be very infrequent.

6.1 Distant sources

Two scenarios were selected on the basis that they were likely to cause inundation with a spatial extent that is representative of the 100 year and 500 year return time inundation from distant source earthquakes. While it is intended that the general pattern of inundation in these scenarios should be approximately representative of these return times, many of the details - such as the timing and number of waves – are unique to the specific scenarios chosen.

6.1.1 100 year event – M_W 9.1 earthquake in Peru

The methodology of the Berryman (2005) report was used to estimate the median 100 year zero-peak wave-height in Gisborne from distant sources. This was calculated to be 2.8m. According to the source-parameterisation used in the Berryman (2005) report a wave of this height can be expected following an earthquake of M_W 9.1 on the Peru coast. Consequently an earthquake of this magnitude, centred at location (14.4°S, 77.2°W) near Pisco in Peru was used as the source for this scenario. The recurrence interval for earthquakes of this magnitude that occur specifically on the Peru coast is about 650 years.

This scenario shares many features with the 1868 Peru tsunami (same magnitude and similar location). This tsunami was observed by early European settlers of Poverty Bay, but information is limited. The scenario is also likely to be similar in its consequences to the 1960 Chile earthquake, which was of a larger magnitude M_W 9.5, but directed a smaller proportion of its tsunami energy towards New Zealand. That tsunami caused disruption to the wharves in the port area of Gisborne and sent surges up the rivers, but caused little inundation.

6.1.2 500 year event – M_W 9.4 earthquake in Peru

The methodology of the Berryman (2005) report was used to estimate the median 500 year zero-peak wave-height from distant sources. This was calculated to be 6.6m. According to the source-parameterisation used in the Berryman (2005) report a wave of this height can be expected following an earthquake of M_W 9.4 on the Peru coast. Consequently an earthquake of this magnitude, centred at location (14.4°S, 77.2°W) near Pisco in Peru was used as the

source for this scenario. No comparable event is recorded in New Zealand written history. The recurrence interval for earthquakes of this magnitude that occur specifically on the Peru coast is about 3500 years.

6.2 Local sources

Scenarios 6.2.1-6.2.3 are based upon earthquake source models in the New Zealand Seismic Hazard Model (NZSHM). The NZSHM allows for uncertainty in the fault geometry and the magnitude and frequency of earthquakes. The scenarios used here are based upon the best ('preferred' in the terminology of the NZSHM) estimate of the fault geometry, but assume the maximum amount of single event displacement permitted in the NZSHM. The quoted recurrence intervals are based upon the preferred NZSHM estimate of the fault recurrence.

The three faults considered in scenarios 6.2.1-6.2.3 are likely to intersect with the plate interface at their lower edge, and it is considered possible that a rupture on these faults may be accompanied by slip on the part of the plate interface that is deeper than this intersection. Scenario 6.2.4 is based on such an event occurring at the Lachlan Fault.

6.2.1 Lachlan Fault

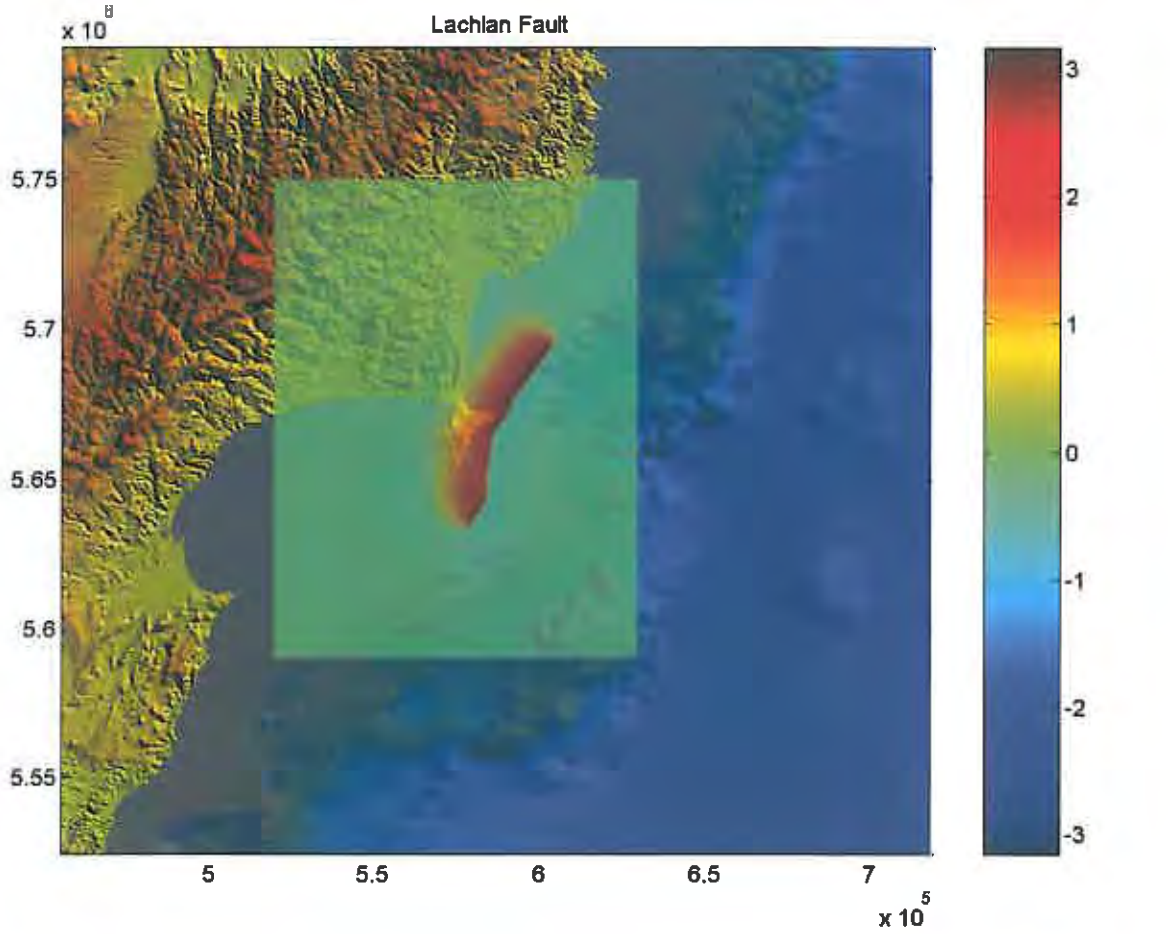

Figure 6.2.1-1 Uplift distribution for the Lachlan Fault source model. The scale bar is in meters, and the pale box indicates the extent of the deformation model.

The Lachlan Fault source model is based on data from the New Zealand Seismic Hazard Model. The rupture is assumed to take place on 7 fault-plane segments with a total length of 69 km. The fault is assumed to dip at 40° over a width of 19 km starting from a depth of 500 m. The preferred recurrence interval for this fault is 930 years. The rupture dislocation is assumed to be 5.3 m, corresponding to a magnitude of M_W 7.6. The calculated seabed deformation is shown in Figure 6.2.1-1.

6.2.2 Ariel Bank Fault

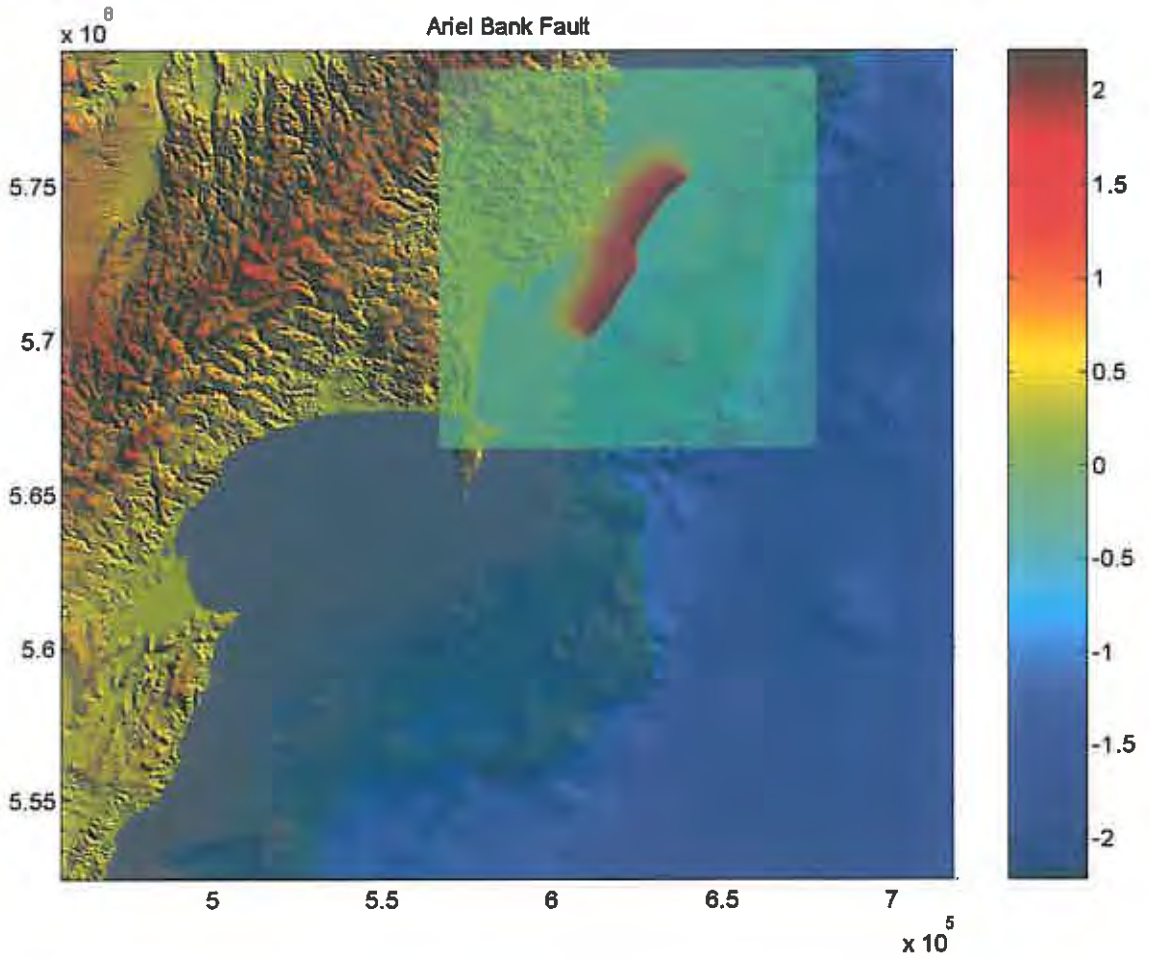

Figure 6.2.2-1 Uplift distribution for the Ariel Bank Fault source model. The scale bar is in meters, and the pale box indicates the extent of the deformation model.

The Ariel Bank Fault source model is based on data from the New Zealand Seismic Hazard Model. The rupture is assumed to take place on 6 fault-plane segments with a total length of 62 km. The fault is assumed to dip at 40° over a width of 19km starting from a depth of 500 m. The preferred recurrence interval for this fault is 630 years. The rupture dislocation is assumed to be 4.8 m, corresponding to a magnitude of M_W 7.5. The calculated seabed deformation is shown in Figure 6.2.2-1.

6.2.3 Gable End Fault

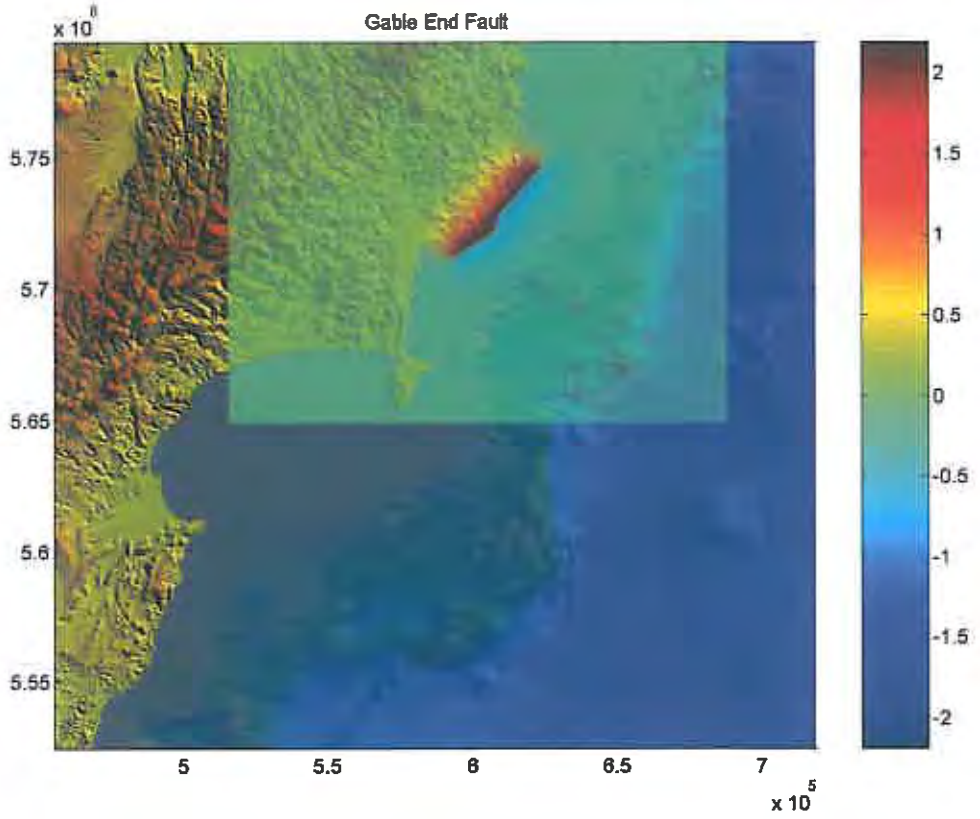

Figure 6.2.3-1 Uplift distribution for the Gable End Fault source model. The scale bar is in meters, and the pale box indicates the extent of the deformation model.

The Gable End Fault source model is based on data from the New Zealand Seismic Hazard Model. The rupture is assumed to take place on 4 fault-plane segments with a total length of 48 km. The fault is assumed to dip at 60° over a width of 17 km starting from a depth of 500 m. The preferred recurrence interval for this fault is 760 years. The rupture dislocation is assumed to be 3.7m, corresponding to a magnitude of M_W 7.4. The calculated seabed deformation is shown in Figure 6.2.3-1.

6.2.4 Lachlan Fault + deeper plate interface

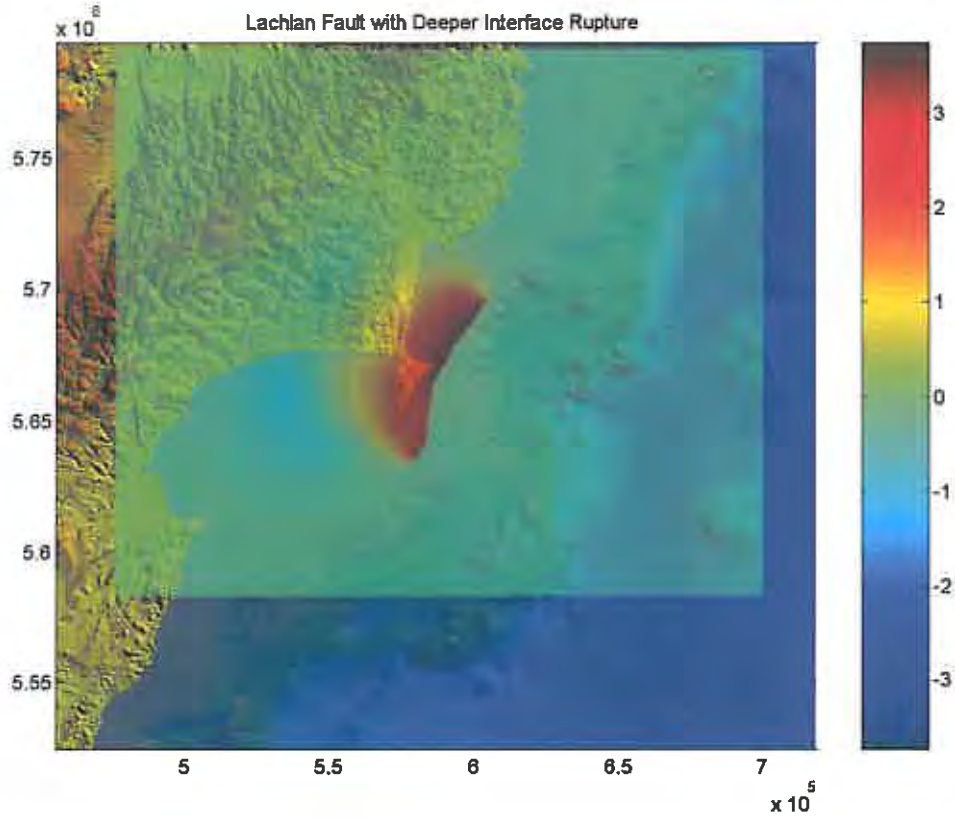

Figure 6.2.4-1 Uplift distribution for the Lachlan Fault with deeper interface rupture source model. The scale bar is in meters, and the pale box indicates the extent of the deformation model.

For the Lachlan Fault and Deeper Plate Interface source model, it was assumed that rupture on the Lachlan Fault takes place down to the depth where the Lachlan Fault meets the plate interface, and is accompanied by slip on the part of the plate interface deeper than this intersection.

The rupture is assumed to take place on 7 fault-plane segments of the Lachlan Fault, and 7 corresponding segments of the deeper plate interface, with a total length of 69 km. The Lachlan Fault is assumed to dip at 40° over a width of 19 km starting from a depth of 500 m, and the Plate Interface rupture is assumed to dip at 8.5° over a width of 34 km. The rupture dislocation is assumed to be 5.3 m, corresponding to a magnitude of M_W 7.9. The calculated seabed deformation is shown in Figure 6.2.4-1.

The preferred recurrence interval for earthquakes on the Lachlan Fault is 930 years, but it is not known what proportion of earthquakes on the Lachlan Fault are accompanied by slip on the deeper plate interface.

6.2.5 Whole margin plate interface M_W 9.0

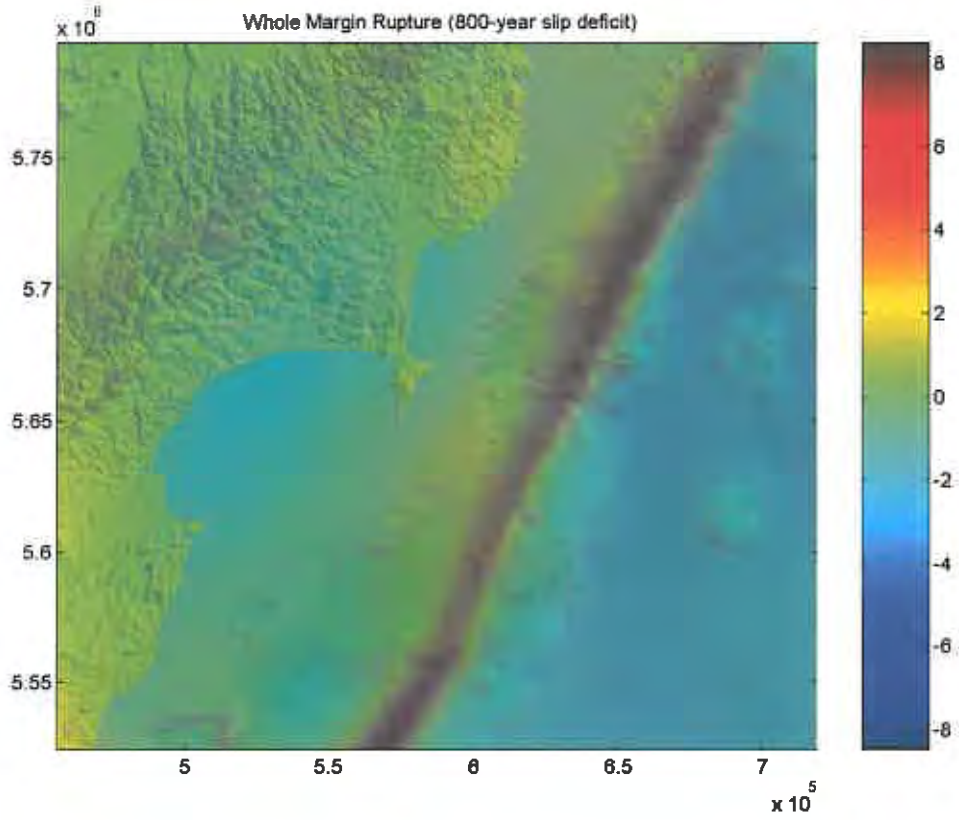

Figure 6.2.5-1 Uplift distribution for the Whole margin rupture M_W 9.0 source model. Only the part of the uplift distribution which occurs within our modelling domain is shown here. The scale bar is in meters, and the pale box indicates the extent of the deformation model.

The whole margin plate interface M_W 9.0 scenario represents a plausible worst case for earthquakes on the Hikurangi subduction zone. In this scenario the entire plate interface from Cook Strait to East Cape ruptures in a single great event (Full details are in Power et al, 2008, Section 3.6). Studies of subduction zones with long historical records have shown that while large plate interface thrust events tend to recur in specific segments of the plate boundary, periodically two or more segments will rupture simultaneously, resulting in a great earthquake (e.g. Ando, 1975). Similarly, paleoseismic results suggest that although the Cascadia subduction zone shows evidence of rupture segmentation, the preferred rupture mode for events of at least *M* ~8 or larger is for full or nearly full margin rupture (Goldfinger et al., 2006).

The rupture in this scenario is assumed to propagate up to a minimum depth of 5 km, and to extend along the entire length of the Hikurangi margin. The scenario earthquake is of M_W = 9.0[2]. The calculated seabed deformation is shown in Figure 6.2.5-1. The Poverty Bay area is subsided by about 0.3 to 0.8 meters. The subsidence is larger further to the southwest, up to 1.7 meters in Hawke Bay.

[2] To derive this scenario it was assumed that 800 years of accumulated slip deficit, as currently estimated using GPS, is released along the Hikurangi margin. This should not be confused with an event of 800 year recurrence interval because: the rate of slip deficit accumulation may vary over the interval between earthquakes, some slip will be released in more frequent smaller earthquakes, and because it is not known how much slip deficit can accumulate before an earthquake occurs.

It is unclear whether such an earthquake rupture can extend into the Poverty Bay region, as it may be the case that frequent smaller earthquakes, such as those in 1947, prevent sufficient stress from being accumulated for such an event to take place; but the possibility cannot be ruled out. It is also possible that stress drops from such smaller earthquakes may make such large events highly infrequent.

The recurrence interval for this scenario is at least 800 years, and may be much longer than this. It is possible that such large events do not ever occur on this subduction zone.

6.2.6 Whole margin plate interface M_W 8.8

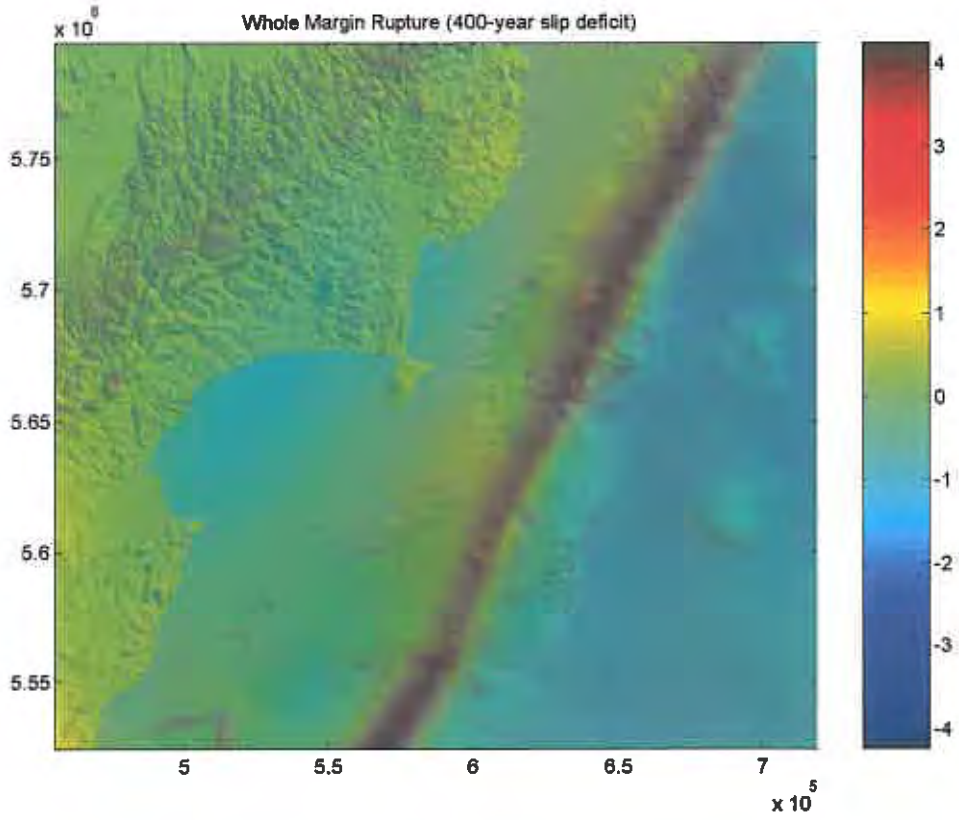

Figure 6.2.6-1 Uplift distribution for the Whole margin rupture M_W 8.8 source model. Only the part of the uplift distribution which occurs within our modelling domain is shown here. The scale bar is in meters, and the pale box indicates the extent of the deformation model.

The Whole Margin plate interface M_W 8.8 scenario is a variation on the M_W 9.0 scenario (6.2.5) in which the slip dislocation has been halved, corresponding to an accumulated slip deficit in 400 years. All other parameters remain the same. The calculated seabed deformation is shown in Figure 6.2.6-1.

6.2.7 Outer Rise M_W 8.0

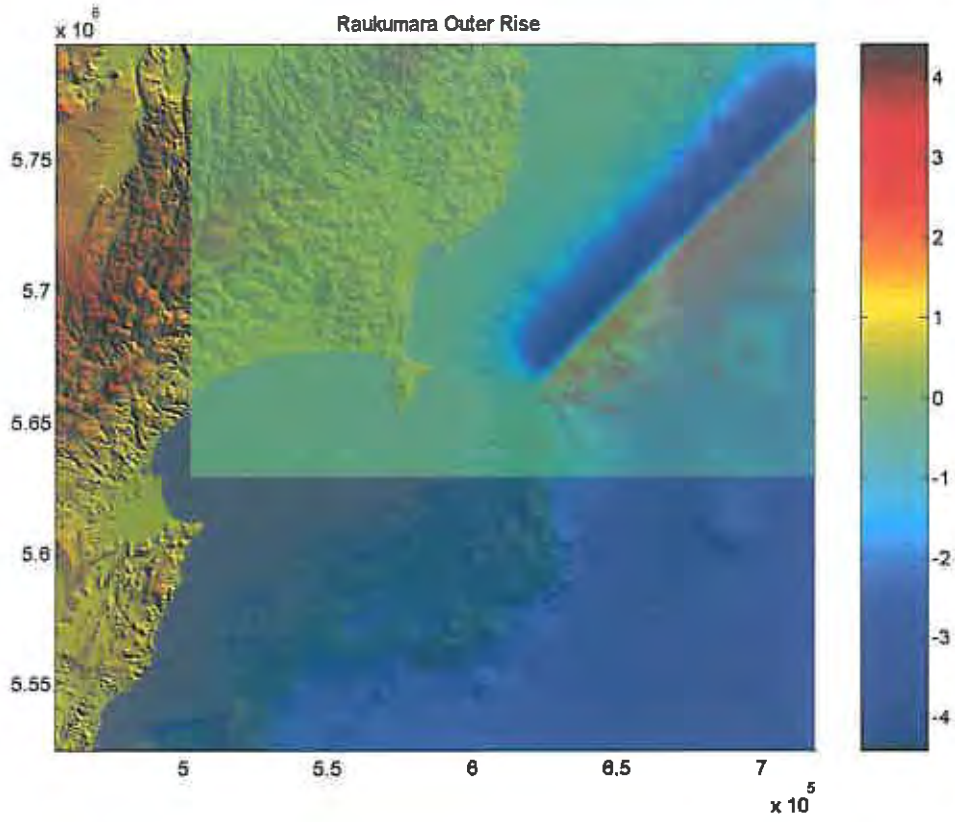

Figure 6.2.7-1 Uplift distribution for the Raukumara Outer Rise source model. The scale bar is in meters, and the pale box indicates the extent of the deformation model.

This scenario assumes an M_W 8.0 earthquake in a similar location relative to the trench as the M_W 7.1 Waitangi Day earthquake of 1995. The event is located between East Cape and Mahia Peninsula, and is considered a worst case scenario for an outer rise event in this area. The rupture length is 150 km, and width is 30 km (scaled from M_W 8.3 1977 Sumba earthquake). The fault dips 58° to NW (similar to the 1995 earthquake). The average slip is assumed to be 8 m, and the estimated recurrence interval for such a source is 1300 years (Power et al, 2008, Section 3.5). The estimated seabed deformation is shown in Figure 6.2.7-1.

6.2.8 Gisborne segment rupture

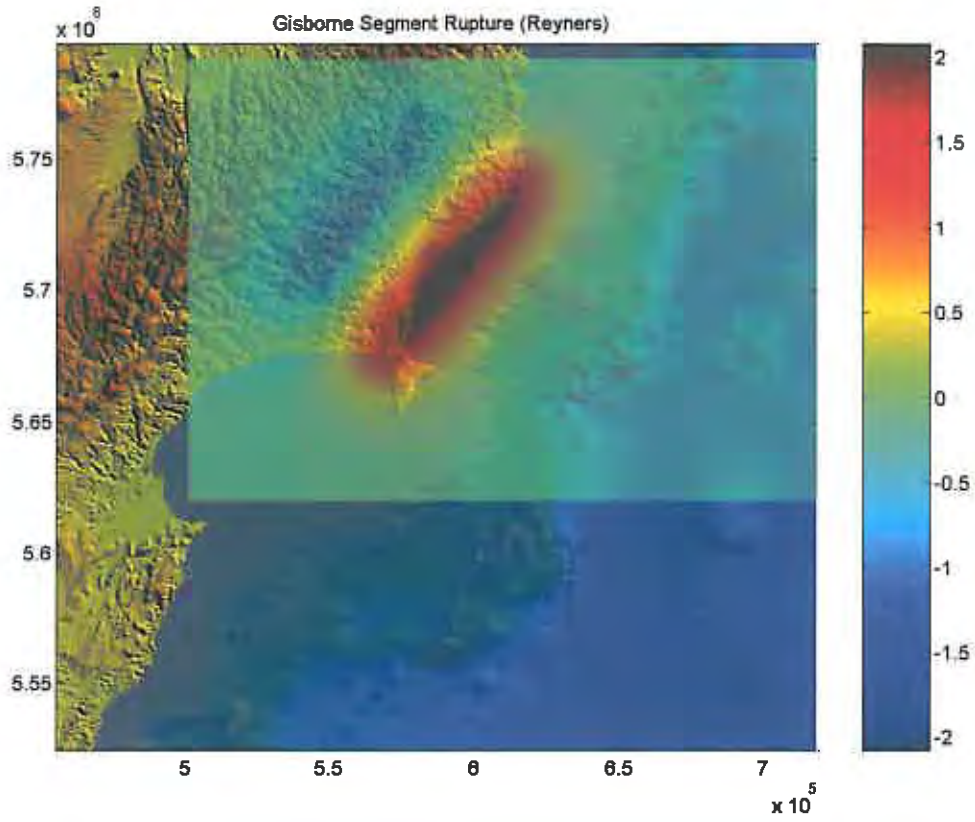

Figure 6.2.8-1 Uplift distribution for the Gisborne segment rupture source model. The scale bar is in meters, and the pale box indicates the extent of the deformation model.

The Gisborne segment rupture scenario is based on the estimates of the seismogenic zone of the plate interface by Reyners (1998), and is scenario 3.4.1 of Power et al (2008). This assumes a rupture on the plate interface of a segment dipping at 10°, starting from 15 km depth and dropping to 22 km depth. Displacement of this segment is assumed to be 6.4m, corresponding to a magnitude M_W 7.8.

Parameters for this scenario of a rupture on the Gisborne segment:

- Deeper edge @ 22 km depth, endpoints 38.96°S 177.45°E, 38.25°S 178.08°E;
- Shallower edge @ 15 km depth, endpoints 39.13°S 177.75°E, 38.41°S 178.38°E;
- Average slip 6.4 m; average recurrence at ~ 52 mm/year (Wallace et al. 2004) is 123 years.
- The fault plane dips at 10 degrees here.

This is an M_W 7.8 event with a recurrence interval of at least 123 years (this lower bound assumes full coupling of the plate interface, and that slip on this part of the plate interface is only released in events of this type, the recurrence interval will be longer if slip is also released here in accompaniment with earthquakes on local faults such as the Lachlan and Ariel Bank Faults).The estimated seabed deformation is shown in Figure 6.2.8-1.

6.2.9 Interface rupture based on GPS coupling

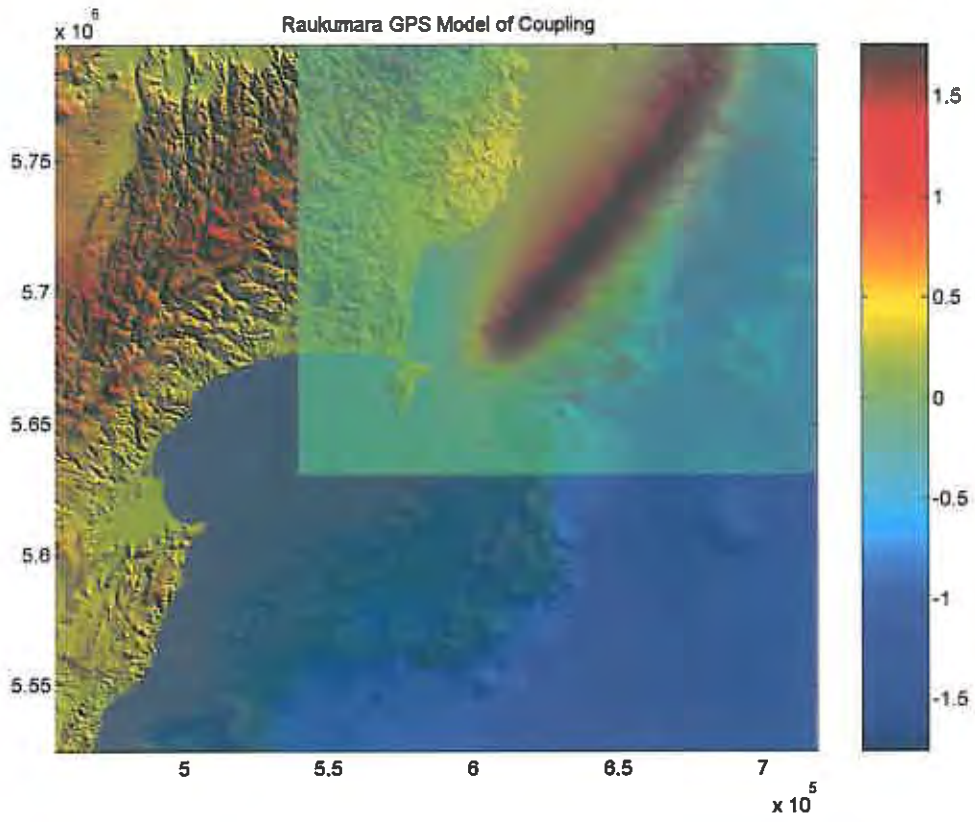

Figure 6.2.9-1 Uplift distribution for the Raukumara GPS model coupling source model. The scale bar is in meters, and the pale box indicates the extent of the deformation model.

The Interface rupture based on the GPS coupling scenario is based on scenario 3.4.3 of Power et al (2008). The slip rate deficit model of Wallace et al. (2004) and Wallace and Beavan (2006) was used to determine the coseismic slip in this scenario. In this model, the accumulated slip (i.e., slip deficit) between the plate interfaces was derived from the GPS measurements on the tectonic plate displacement near the plate interface. The slip deficit accumulated in a 400 year interval at current coupling rates was assumed to be released in this scenario earthquake. This is a M_W 8.1 event. In this scenario we extend rupture up to 10 km depth (shallowest part) and the estimated seabed deformation is shown in Figure 6.2.9-1.

7.0 SITE

7.1 Geographic setting

The Gisborne region is located on the East Coast of North Island, New Zealand (Figure 7.1-1). The region includes Poverty Bay that opens to the southeast and extends from Young Nicks Head in the south to Tuaheni Point (~ 8.5 km wide) in the northeast. The Gisborne City

Centre is located at the northern side of Poverty Bay. There are two major rivers along the coast of Poverty Bay; the Waipaoa River at the southwest of the bay, and the Turanganui River with its port facility at the northern end, where the Taruheru and Waimata Rivers meet. A relatively large shallow lagoon is located immediately to the south of Waipaoa River at the southwestern end of the Bay, namely Wherowhero Lagoon.

Most of the coastal topography of Poverty Bay is flat with cliff formations at the end of the Bay, along both the northern, (Titirangi Domain) and southern ends (Young Nicks Head). There are sand dunes along the coast of non-uniform height. The highest sand dune (5.0 – 6.0 m high and 70 – 100 m wide) is located at the centre part of the Bay (section B), and lower sand dunes are at the southwestern end of the coastal areas from the Wherowhero lagoon (section D) up to the areas around the Waipaoa River mouth (section C), and the areas close to the Port (section A). At section A, the sand dunes heights range from 3.0 – 5.0 m, while section C and D heights are lower, ranging from 2.0 – 4.0 m and up to 2.0 m respectively (Figure 7.1-2)

Poverty Bay shows a mildly sloping nearshore bathymetry fringed with long sandy beaches with patches of shoaling regions close to Young Nicks Head. The greatest water depth of the Bay (~ 25.0 – 30.0 m) is located at the centre of the Bay entrance and from there the bathymetry gradually becomes deeper towards the wide continental shelf and slope, which are located further offshore on the tectonically active northern Hikurangi margin of New Zealand.

Three areas were chosen for the detailed assessment of tsunami inundation dynamics; two inside Poverty Bay (the Gisborne City and Muriwai – Waipaoa Rivers) and one, Wainui, located outside of the Bay, immediately north of Tuaheni Point, and facing the open ocean.

Figure 7.1-1 The Gisborne region located on the East Coast of North Island, New Zealand.

Figure 7.1-2 The Poverty Bay site where detailed inundation studies were carried out. This figure also shows the locations of the 12 virtual tide gauges.

7.2 Virtual tide-gauges

Virtual tidal gauges were deployed in the numerical models to track the arrival times of tsunami and the water surface fluctuations for different scenario events. The UTM coordinates (Zone -60, WGS84 Datum) and water depth of these virtual tidal gauges are given in Table 7.2-1 and Figure 7.1-2. The virtual tide gauges measure the instantaneous water-level relative to Mean Sea Level (the datum and instrument response of real tide gauges are generally more complicated).

Table 7.2-1 Locations of Virtual Tidal Gauges

Gauge No.	X Coordinate (m)	Y Coordinate (m)	Depth (m)
01	585980.0	5710230.0	13.76
02	584480.0	5710730.0	9.45
03	582480.0	5710730.0	3.77
04	582480.0	5713730.0	8.20
05	584480.0	5716730.0	11.94
06	587980.0	5718730.0	6.71
07	589480.0	5716730.0	12.93
08	592980.0	5714230.0	8.09
09	593480.0	5716730.0	2.47
10	586480.0	5713730.0	21.15
11	588980.0	5712230.0	21.38
12	592980.0	5710230.0	30.37